The Shrinkage of Lake Lop Nur in the Twentieth Century: A Comprehensive Ecohydrological Analysis

DANLU CAI,[a,b] LIJUN YU,[a,b] JIANFENG ZHU,[a,b] KLAUS FRAEDRICH,[c] YANNING GUAN,[a] FRANK SIELMANN,[d] CHUNYAN ZHANG,[a,b] AND MIN YU[e]

[a] *Aerospace Information Research Institute, Chinese Academy of Sciences, Beijing, China*
[b] *Joint Laboratory of Remote Sensing Archaeology, Aerospace Information Research Institute, Chinese Academy of Sciences, Beijing, China*
[c] *Max Planck Institute for Meteorology, Hamburg, Germany*
[d] *Meteorologisches Institut, Universität Hamburg, Hamburg, Germany*
[e] *Urban Planning and Design Institute of Shenzhen, Shenzhen, China*

(Manuscript received 27 September 2021, in final form 8 March 2022)

ABSTRACT: A comprehensive ecohydrological analysis is designed to understand the formation and evolution of lake Lop Nur and the environmental change over the Tarim River basin. Three temporal scales from century-based climatological mean to decade-based quasi-steady state change and to annual-scale-based abrupt change test are included. Combining the Budyko and Tomer–Schilling framework, this research first analyzes hydroclimatic and ecohydrological resistance/resilience conditions, then attributes observed changes to external/climate impact or to internal/anthropogenic activities, and finally diagnoses the possible tipping point on ecohydrological dynamics. (i) The arid regions reveal less sensitivity in terms of low variabilities of excess water *W* and energy *U* and show high resilience, which will more likely stay the same pattern in the future. (ii) Present towns situated in the semiarid regions with a natural hydraulic linkage with the mainstream of the Tarim River show a higher sensitivity and likelihood to be affected if drier scenarios occurred in the future. (iii) The attribution from two subsequent quasi-steady states indicates increasing effects of the anthropogenic activities increase (1961–80 versus 1981–2000) and provides climatical evidence that the central Tarim River basin was getting wetter before 1960 and then kept drying afterward. (iv) In the Kongqi subcatchment, the excess water reveals a significant decrease-then-increase evolution, from which the years with abrupt changes are observed in the 1960s. Generally, both points iii and iv are in agreement with that the closed-basin lake Lop Nur desiccation until the 1970s and its connection with the eastern part of the Taklamakan Sand Sea.

KEYWORDS: Atmosphere-land interaction; Climate change; Hydrology; Ecological models; Annual variations

1. Introduction

For climatological averages, the Budyko (1974) framework provides a simple first-order relationship to quantify the rainfall–runoff chain dynamics on watershed scales (Arora 2002; Roderick and Farquhar 2011; Wang and Alimohammadi 2012). The related ecohydrological conceptual model proposed by Tomer and Schilling (2009) utilizes two nondimensional flux ratios (relative excess energy *U* and excess water *W*) as ecohydrological state space variables, diagnosing the causes of hydrological change induced by external/climatic and internal/anthropogenic impacts (see also Cai et al. 2016, 2015; Renner et al. 2012). According to the conceptual model, ecohydrological resistance and resilience are calculated, measuring the degree to which runoff is coupled/synchronized with precipitation, and the degree to which a catchment can return to normal after perturbations (Carey et al. 2010; Creed et al. 2014; Esquivel-Hernández et al. 2017).

However, the ideal rainfall–runoff chain-based ecohydrological analyses assumes quasi-steady states for closed terrestrial water basins, where nonstationary processes are not fully represented (Chen et al. 2013; Greve et al. 2016). This is because the ecohydrological conceptual model is subjected to two physical constraints determined by the limited forcing of water demand and supply (the water demand limit represents sensible heat flux being bound by net radiation whereas the water supply limit determines runoff to be limited by precipitation), where the water and heat storage deficits are neglected. For example, year-to-year changes in soil moisture from transient climate change may be neglected (Orlowsky and Seneviratne 2013; Wang 2005). To address this limitation, the Budyko framework was extended for subannual to annual scale by including additional parameters to be implicitly related to the storage term of the rainfall–runoff chain (Chen et al. 2013; Greve et al. 2016; Potter and Zhang 2007; Zhang et al. 2008). Although these approaches provide empirical or analytical insights on nonstationary processes affecting the Budyko framework, trends, and abrupt changes (or tipping points), which account for climatological changes entering the attribution analysis, are still missing.

The Tarim River basin in central Asia hosts the second-largest sand desert of the world (the Taklamakan Sand Sea), where the precipitation is lower than 20 mm yr^{-1}. However, according to historical documents of the Han Dynasty, the lake in the basin once covered 17 000–50 000 km^2 due to streams from towering mountain ranges in the north, west, and south (Mischke et al. 2017; Yang et al. 2006). Streams

Corresponding authors: Danlu Cai, caidl@radi.ac.cn; Lijun Yu, yulj@aircas.ac.cn

DOI: 10.1175/JHM-D-21-0217.1

flew and charged the closed-basin lake Lop Nur with a surface area more than 2000 km^2 in the early 1930s (Mischke et al. 2020) but eventually desiccated by the 1970s (Hao et al. 2008; Hong et al. 2003; Hörner 1932; Qin et al. 2012). Efforts have been made to demonstrate the sensitivity of the arid and semi-arid regions (Xue et al. 2017), to diagnose the streamflow trend differences upstream and downstream (Xu et al. 2010), and to identify potential impacts of climate change and anthropogenic activities on streamflow alterations (Xu et al. 2013; Xue et al. 2017).

Still, the formation and evolution of lake Lop Nur and the environmental change over the Tarim River basin remain a topic of hot debate (Dong et al. 2012; Hedin 1925; Mischke et al. 2020, 2017; Xue et al. 2017). Therefore, instead of establishing the statistical relationship between streamflow and climatic factors, a comprehensive ecohydrological approach is designed to first analyze hydroclimatic and ecohydrological resistance/resilience conditions, then to attribute observed changes to external/climate impact or to internal/anthropogenic activities, and finally, to diagnose the possible tipping point on ecohydrological dynamics. Note that the external/climate impacts include natural climate variability, global climate change, and the regional climate effects of human activities (Wang and Hejazi 2011), e.g., El Niño–Southern Oscillation, which is an irregular periodic variation in winds and sea surface temperatures over the tropical Pacific Ocean that affects the climate of the tropics and subtropics. Internal/anthropogenic impacts are understood as modification of the interrelation between evapotranspiration and potential evaporation and its effect on the recycling of precipitation (Brutsaert and Parlange 1998; Roderick and Farquhar 2011; Szilagyi 2007).

After introducing the geographical setting and climatological datasets, methods of analysis are presented (section 2). Application over 12 subcatchments of the Tarim River basin, regions with ancient relics versus present towns, are presented, including century-based climatological resistance and resilience, decade-based quasi-steady-state change, and annual-scale-based abrupt change testing (section 3), followed by a concluding summary (section 4).

2. Data description and methodology

Reanalysis records from 1900 to 2010 are downloaded from the ERA-20CM dataset, which contains an ensemble of 10 atmospheric model integrations. The ensemble means of the 10 ensemble members are finally employed to represent the ERA-20CM reanalysis with a horizontal resolution of 0.75° × 0.75°. The model used to generate the reanalysis records considers the land cover changes over the entire period of analyses (Boussetta et al. 2013; Hersbach et al. 2015). The comprehensive ecohydrological approach first quantifies the ecohydrological resistance and resilience from 1901 to 2010 (see also Esquivel-Hernández et al. 2017). Then it revisits subsequent 20-yr time intervals (1901–20 versus 1921–40; 1921–40 versus 1941–60; 1941–60 versus 1961–80; 1961–80 versus 1981–2000) to attribute observed changes to external/climate impact or to internal/anthropogenic activities with the ecohydrological conceptual model from Tomer and Schilling (2009) (see also Cai et al. 2016). After applying the ecohydrological conceptual model to annual scale, the Mann–Kendall (MK) statistical test (Libiseller and Grimvall 2002) has been applied for trend detection of the hydrometeorological attribution time series to explore the possible occurrence of points of changing trends or of tipping points for further understanding the ecohydrological dynamics.

a. Ideal rainfall–runoff chain

Land climates on catchment scale are controlled by water supply and demand, represented by the precipitation P and net radiation N (or potential evapotranspiration). Long-term area-averaged water and energy fluxes satisfy the flux balance equations, that the precipitation P is balanced by runoff Ro and evapotranspiration E, while the net radiation N is balanced by sensible heat flux H and evapotranspiration E:

$$\text{Water supply: } P = \mathrm{Ro} + E,$$

$$\text{Energy supply: } N = H + E.$$

b. The ecohydrological state space

Following Tomer and Schilling (2009), a separation of energy and water fluxes characterizes the ecohydrological environment in terms of relative excess water W and relative excess energy U. Relative excess water W is the portion of water supply not being used by the ecosystem and thus available for geomorphological formation, while relative excess energy U is the portion of energy supply not being used for evapotranspiration and thus available for photosynthesis:

$$W = \mathrm{Ro}/P = 1 - E/P,$$

$$U = H/N = 1 - E/N.$$

c. Dryness ratio

Dryness combines energy and water fluxes into one parameter relating water demand (energy supply) to water supply:

$$D = N/P = (1 - W)/(1 - U).$$

The range of dryness ratio $D < 1$ characterizes energy limited climates and $D > 1$ for water limited regimes [for its stochastic interpretation as an ideal rainfall–runoff chain or equation of state, see Fraedrich (2010)].

d. Resistance and resilience

The resistance and resilience are calculated using the standard deviation (σ) in U and W in long-term period (n; see also Esquivel-Hernández et al. 2017) as follows:

$$\sigma U = \sqrt{\frac{1}{n-1}\sum_{i=1}^{n}(U_i - \overline{U})^2},$$

$$\sigma W = \sqrt{\frac{1}{n-1}\sum_{i=1}^{n}(W_i - \overline{W})^2}.$$

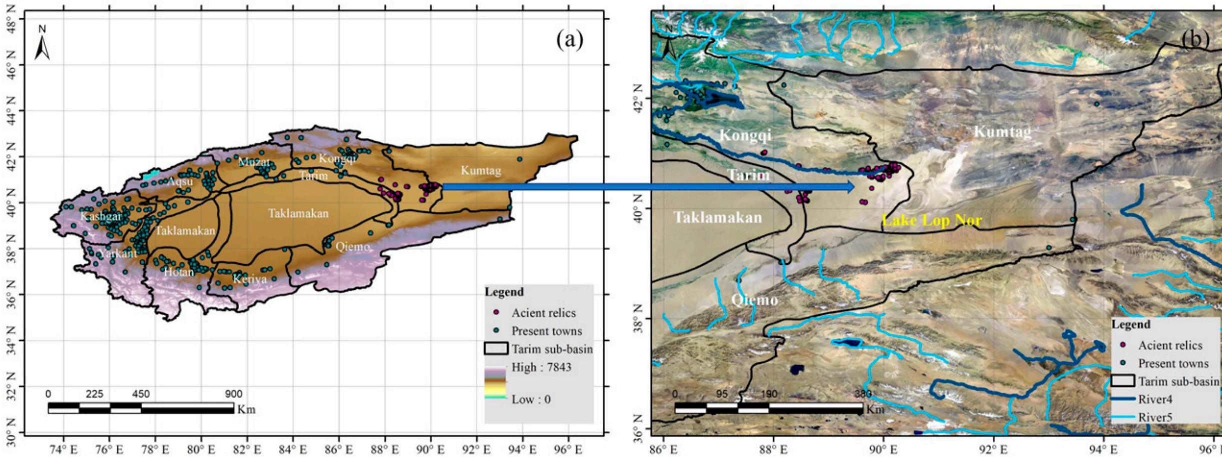

FIG. 1. Geographical setting of (a) the Tarim River basin, 12 subcatchments, regions with ancient relics vs present towns and (b) lake Lop Nor. Subcatchments' boundary information (Xu 2019) is downloadable from https://data.tpdc.ac.cn/zh-hans/.

The hydrological resistance (σW) measures the synchronicity between the partitioning of precipitation into runoff in a catchment (Creed et al. 2014), and resilience ($\sigma U/\sigma W$) measures hydrological elasticity, that is, the degree of a catchment returning to normal functioning as response to hydroclimatic perturbations (Carey et al. 2010; Creed et al. 2014).

e. Ecohydrological attribution

External/climate impact (CT) and internal/anthropogenic activities (AT) can now be quantified by trajectories in the ecohydrological (U, W) state space. States shifting from one (long term) averaging period to the next provide a direct measure of the causes of change induced by external (climate) forcing and internal (anthropogenic) processes. Note that the climate state of the first period represents the reference stationary, naturally occurring climate fluctuations moving up and down the axis perpendicular to the first period dryness D_1 line, while anthropogenic activities driving the trajectories away from the line perpendicular to the D_1 line [for a detailed description see Cai et al. (2016)]:

$$\begin{pmatrix} dW' \\ dU' \end{pmatrix} = \begin{bmatrix} \cos(\theta - 45^\circ) & \sin(\theta - 45^\circ) \\ -\sin(\theta - 45^\circ) & \cos(\theta - 45^\circ) \end{bmatrix} \times \begin{pmatrix} W_2 - W_1 \\ U_2 - U_1 \end{pmatrix},$$

$$\begin{pmatrix} \mathrm{CT} \\ \mathrm{AT} \end{pmatrix} = \begin{bmatrix} \cos(\theta - 90^\circ) & \sin(\theta - 90^\circ) \\ -\sin(\theta - 90^\circ) & \cos(\theta - 90^\circ) \end{bmatrix} \times \begin{pmatrix} W_2 - W_1 \\ U_2 - U_1 \end{pmatrix}.$$

Geographically, the catchment is associated with four conditions of change depending on the dynamics of (dW', dU') panel: 1) internal/anthropogenic-induced changes, both dW' and dU' increase (pink first quadrant) or decrease (light blue third quadrant), and 2) external/climate-induced changes, increasing dW' and decreasing dU' (dark blue fourth quadrant) or the converse (yellow second quadrant).

To diagnose the climatological tendency and tipping points within the long-term steady states, besides time series of climatic parameters, the flux ratios of the (W, U) panel, the year-to-year magnitudes of the (dW', dU') panel, and the (CT, AT) panel are also included for a further MK statistical test, so that the possible trends and the tipping points are explored.

f. Mann–Kendall statistical test

The MK test (Libiseller and Grimvall 2002; Mann 1945), a nonparametric method for detecting trends and abrupt changepoints in time series without requiring normality or linearity, has been widely applied in hydrometeorological time series, such as streamflow, precipitation, and temperature [details and advantages of this method, see, e.g., Xu et al. (2010)]. In the following application, time series passing the significance test, p value less than 0.01 will be highlighted for further calculating the tipping point (unless noted otherwise) to reduce errors or leakage test from hydrological nonstationary processes in annual scale.

3. Analyses and discussion

The Tarim River basin (see Fig. 1a), as the largest inland river basin in China, is typically a closed, independent, and self-balanced hydrological system (Leiwen et al. 2005; Ye et al. 2006). Streamflow of the Tarim River basin is mainly generated by precipitation, glacial, and snowmelt water (Changchun et al. 2008; Chen et al. 2007). Except Hotan River, Yarkant River, Aksu River, and Kaidu–Konqi River, which have a natural hydraulic linkage with the mainstream of the Tarim River, most of the river systems of the Tarim River basin were gradually changed or have dried up, losing their relationship with the Tarim River (Xu et al. 2010). To improve our understanding of the formation and evolution of lake Lop Nur (see Fig. 1b) and the environmental change over the Tarim River basin, the comprehensive ecohydrological analysis includes three temporal scales from century to decadal to annual scale. Twelve subcatchments of the Tarim River basin, regions with ancient relics versus present towns, are also selected to employ the tools introduced in the previous section, for 1) comparing the hydrological changes over different subcatchments,

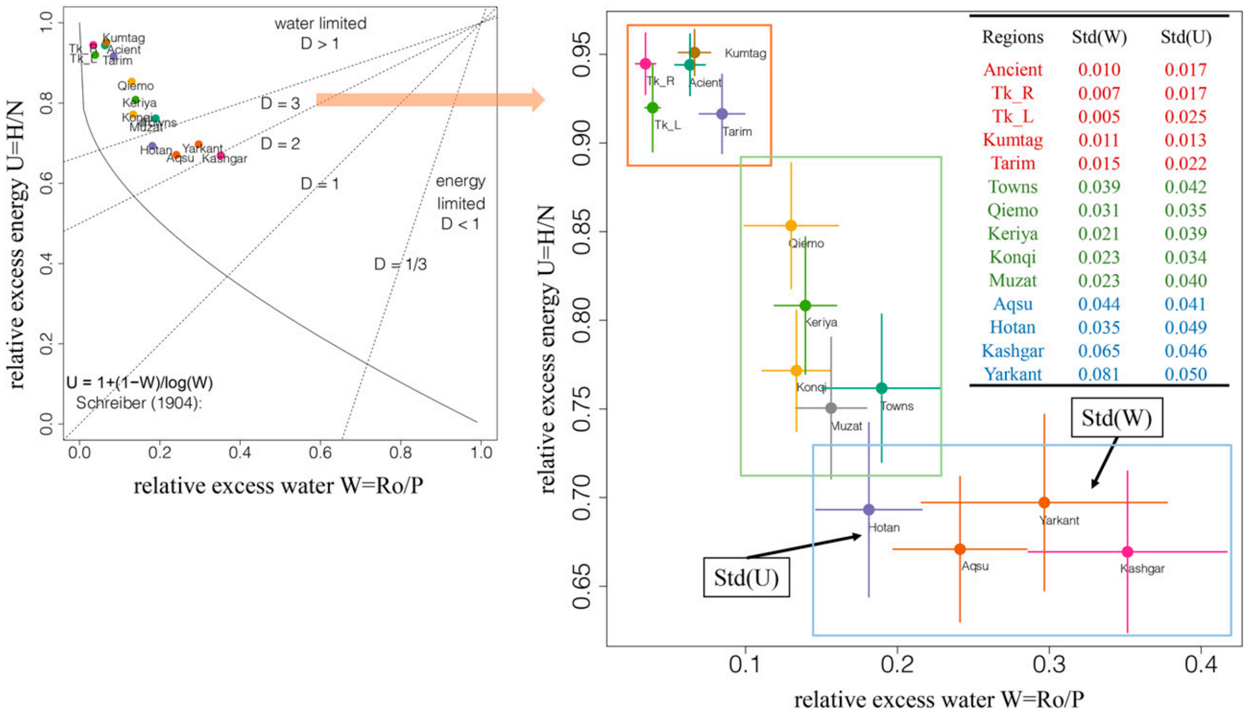

FIG. 2. The ecohydrological states in the (U, W) diagram spanned by relative excess water W (runoff vs precipitation) and energy U (sensible heat flux vs net radiation) with lines of constant dryness D (net radiation vs precipitation): the distribution of 12 subcatchments, regions with ancient relics vs present towns, in terms of first and second moment.

2) diagnosing the possible hydrological differences between ancient and present high population density regions, and 3) further understanding the shrinkage of Lop Nur and its final desiccation in the twentieth century.

a. Ecohydrological resistance and resilience (1900–2010)

The first moments or means of relative excess water W and excess energy U for the time period of 1900–2010 are presented in Fig. 2. A clear separation related to the dryness ratio D could be noticed (see colored boxes):

(i) Subcatchments of Taklamakan, Kumtag, Tarim, and ancient relics/towns (in the red box) with the highest averaged dryness ratio are situated in regions with low relative excess water W and high relative excess energy U, where relative excess water W (relative excess energy U) is less than 0.1 (greater than 0.9).

(ii) Subcatchments of Qiemo, Keriya, Kongqi, Muzat (in the green box), and present towns occupy regions with the second-highest averaged dryness ratio aligned along a constant relative excess water W = ~0.15, meanwhile their relative excess energy U is greater than 0.7.

(iii) Subcatchments of Hotan, Aqsu, Yarkant, and Kashgar (in the blue box) with the averaged dryness ratio D less than 3 are located along a constant relative excess energy U = ~0.68.

(iv) The comparison between regions with ancient and present towns indicates that ancient towns nowadays share a similar ecohydrological situation in terms of excess water W and energy U as the Taklamakan Desert, while present towns are located in regions characterized by a ~0.1 increase (decrease) in relative excess water W (relative excess energy U).

The second moments or standard deviations of excess water W and energy U for the time period of 1900–2010 also indicate a clear separation related to the dryness ratio D (the three colored boxes). In general, regions with more moisture show a higher variability in terms of the standard deviation of excess water W and energy U, which increase as the dryness ratio decreases (Fig. 2). This is precisely represented in terms of the coefficients of variation (Fig. 3):

(i) A positive relationship between the standard deviation of excess water [std(W)] versus excess water W and a negative relationship between the standard deviation of excess energy [std(U)] versus excess energy U could be noticed with a slope of 0.22 and −0.11, respectively (Figs. 3a,b).

(ii) Likewise, a positive relationship between excess water W versus the coefficient of variation of excess water coef(W) = std(W)/W, and a negative relationship between excess energy U versus the coefficient of variation of excess energy coef(U) = std(U)/U could be observed with a slope of 0.21 and −0.18, respectively (Figs. 3c,d).

(iii) The frequency distribution over 12 subcatchments of the Tarim River basin, regions with ancient relics versus present towns, in the diagrams are characterized by two modes separated by excess energy U around 0.85 (see also the red box in Fig. 2) separating arid and semiarid regimes.

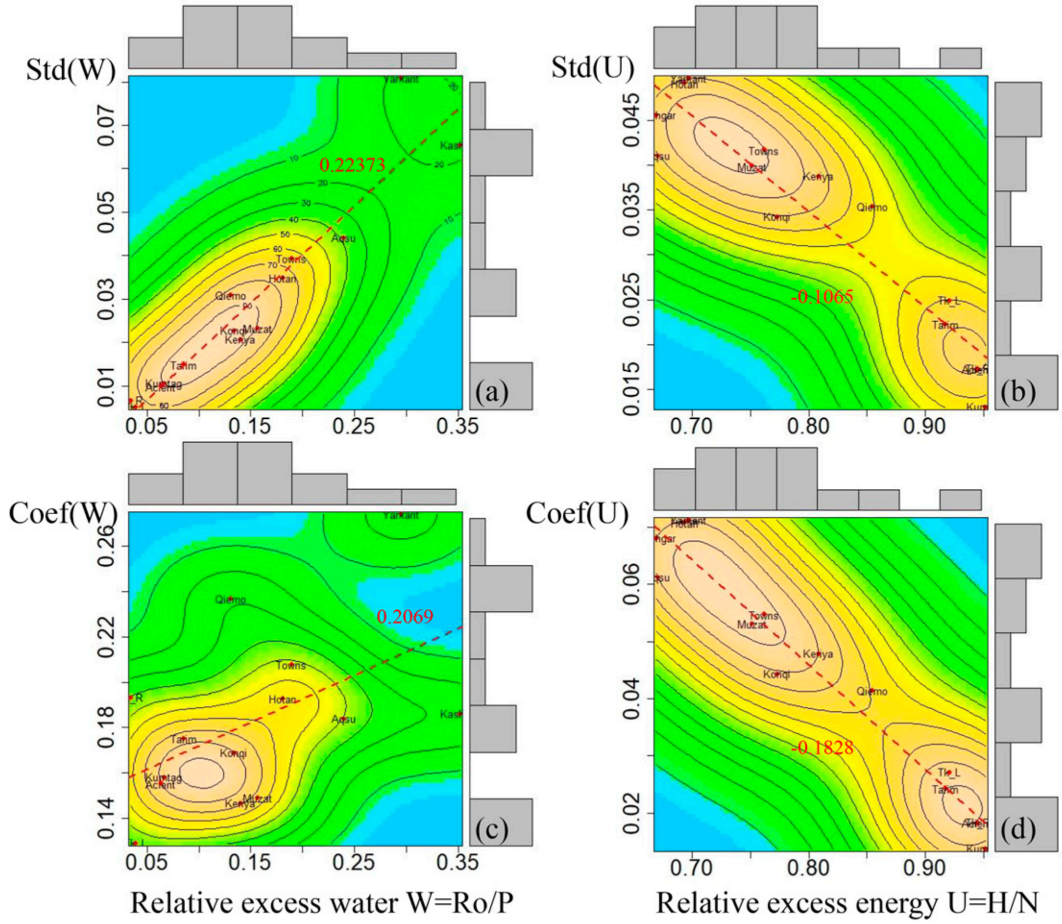

FIG. 3. Frequency distribution of the 12 subcatchments, regions with ancient relics vs present towns, in the (a) [W, Std(W)] diagram, (b) [U, Std(U)] diagram, (c) [W, Coef(W)] diagram, (d) [U, Coef(U)] diagram.

Ecohydrological resistance and resilience are calculated and displayed in Fig. 4 to measure the degree to which runoff is coupled/synchronized with precipitation, and the degree to which a catchment can return to normal after perturbations. The results are noted as follows: regions with more moisture or less dryness ratio show a higher resistance, Yarkant > Kashgar > Aqsu > present towns > Hotan > Qiemo with values 0.081 > 0.065 > 0.044 > 0.039 > 0.035 > 0.031, etc. Unsurprisingly the desert region of Taklamkan and ancient towns indicate the lowest resistance, because resistance measures the degree to which runoff is coupled/synchronized with precipitation. Contrarily, regions with more moisture or less dryness ratio show a lower resilience in the Tarim River basin, Yarkant < Kashgar < Aqsu < present towns with values 0.61 < 0.7 < 0.93 < 1.06, etc. That is, the semiarid regions are more sensitive and likely to be affected if drier scenarios occurred in the future.

b. *Attribution: Quasi-steady state with subsequent 20-yr time intervals*

Regions of significant change from subsequent 20-yr time intervals are qualitatively attributed to external and internal causes by first partitioning the direction of change in state space into four quadrants and displayed geographically (see Fig. 5). Note that regions of (U, W) changes exceeding std(U) or std(W) are considered as significant regions of change. The following results are noted:

(i) Most regions passing the significance test are located in the central arid regions of the Tarim River basin around Taklamakan, due to their relatively larger (U, W) changes and their relatively lower variability std(U) or std(W).

(ii) Attribution in significant regions is predominantly caused by external processes (>60%, second or fourth quadrant, yellow or dark blue) in the subsequent 20 years' comparison. Particularly for the periods of 1921–40 versus 1941–60 and 1941–60 versus 1961–80, external processes control regions more than ~98% of these regions. However, the second period of 1941–60 indicates more moisture caused by external processes compared with the first period (1921–40), while the second period of 1961–80 indicates a drying pattern caused by external processes compared with the first period (1941–60). That is, the central arid regions of the Tarim River basin indicate a dry–wet–dry pattern before and after the 1940s and after the 1960s.

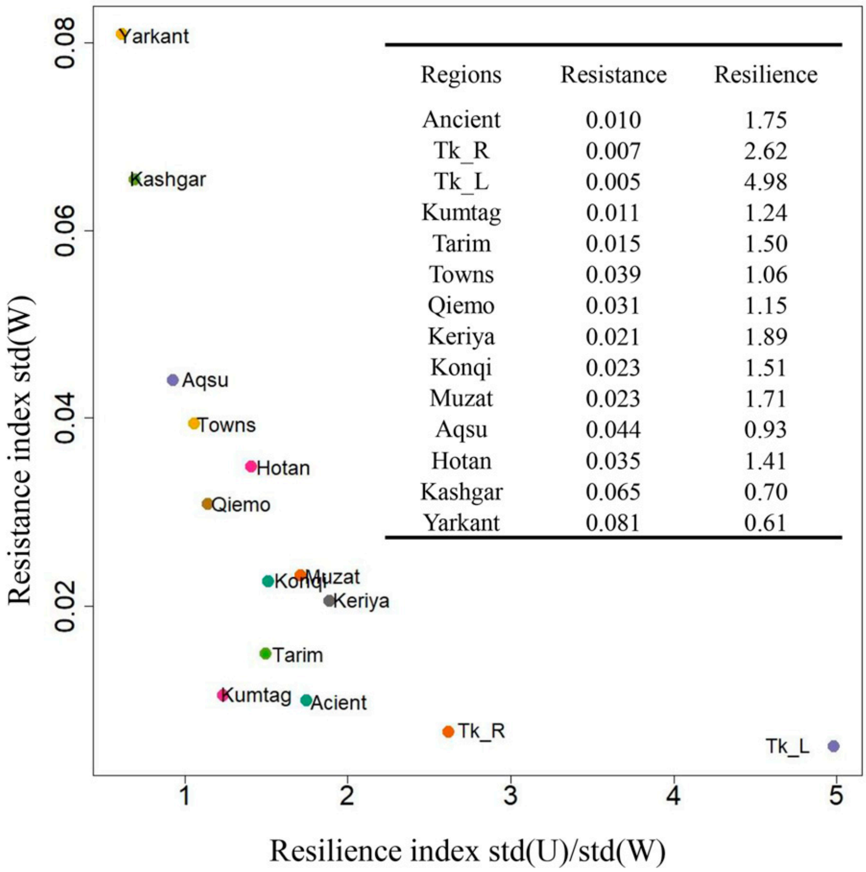

FIG. 4. Surface resistance and resilience state space spanned by the ratio of standard deviation of excess energy U to standard deviation of excess water W, and standard deviation of excess water W. Twelve subcatchments, regions with ancient relics vs present towns, are compared.

(iii) The central arid regions of the Tarim River basin around Taklamakan are predominantly controlled by external processes, while the surrounding regions indicate internal (first or third quadrant, pink or light blue) induced changes, particularly for the periods of 1901–20 versus 1921–40 and 1961–80 versus 1981–2000, accounting for 28.12% and 39.62%, respectively. That is, anthropogenic causes increased by 11.5% compared with the periods of 1901–20 versus 1921–40, and even higher compared with the other two attribution periods. This relates to the rapid population growth from ~3 million in 1949 to ~8.5 million in 2000 (see Zhang et al. 2010), accelerated reclamation, and large irrigation diversions in the Tarim River basin (Chen et al. 2011; Yang and Lu 2014). By 2005, more than one-third of the main streamflow was withdrawn for irrigation, leading to sharp decrease in lake level (Chen et al. 2011).

Time evolution for the periods of 1901–20, 1921–40, 1941–60, 1961–80, and 1981–2000 is represented as a flow in the ecohydrological space and displayed by pieces of trajectories. Twelve subcatchments of the Tarim River basin, regions with ancient relics versus present towns, are compared in Fig. 6. The trajectories of arid regions (Taklamakan, Kumtag, Tarim, and ancient relics/towns, for example) move up and down with a slight change in terms of relative excess water W. That is, time evolution in arid regions occurs mainly due to the changes of local sensible heat flux H, supposing that local net radiation remains stationary in a 20-yr average. The trajectories of semiarid regions indicate movements both vertically and horizontally. This is in agreement with Fig. 2, which shows that, compared with the arid regions, the semiarid regions are more sensitive and likely to be affected by water availability.

c. *Ecohydrological tendency and tipping point: Annual scale time series*

The ecohydrological model was extended for annual scale so as to diagnose the tendency and tipping point of the rainfall–runoff chain by including Mann–Kendall test (p value less than 0.01 is considered as significant abrupt change). The annual time series (1901–2010) subjected to the Mann–Kendall test consist of (i) the five climate variables of precipitation P, evaporation E, sensible heat flux H, net radiation N, and runoff Ro; (ii) the two flux ratios of excess water W and energy U (see appendix); (iii) the changes of the excess water dW and energy dU; and (iv) attribution quantifications of external C or internal

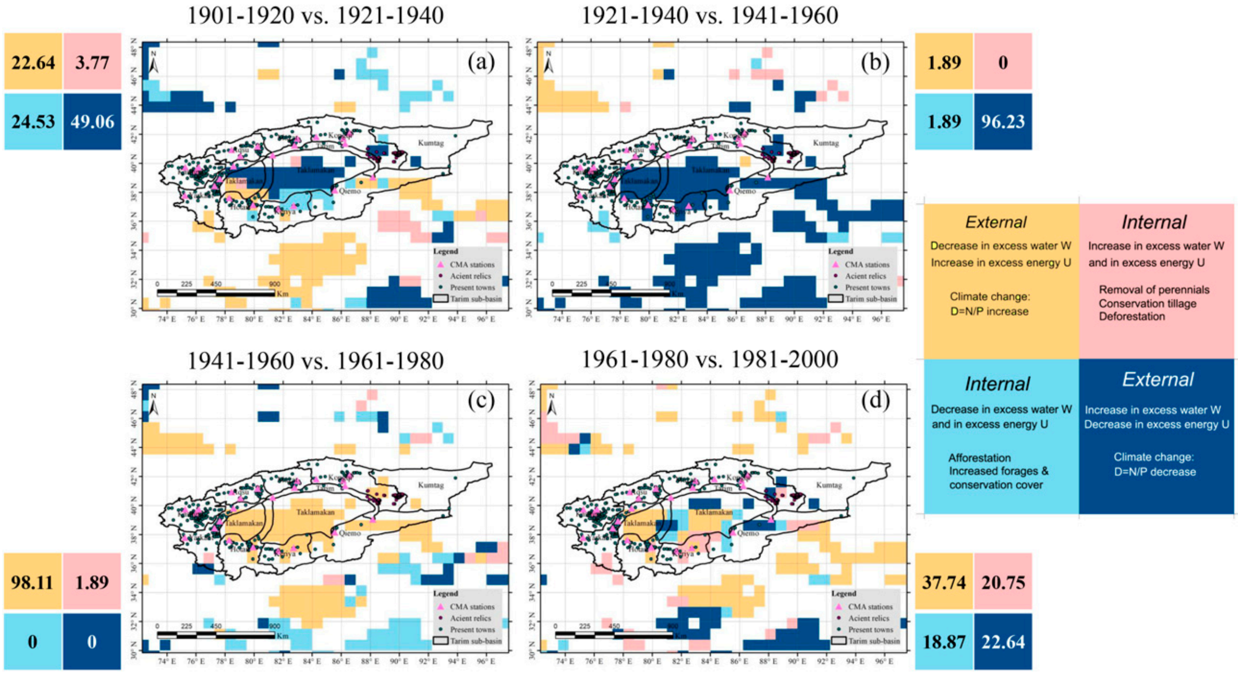

FIG. 5. Distributions of attribution classes of ecohydrological change in Tarim River basin separating internal from external causes: geographical distributions and statistics of (a) 1901–20 vs 1921–40; (b) 1921–40 vs 1941–60; (c) 1941–60 vs 1961–80; (d) 1961–80 vs 1981–2000.

causes *A*. From the arid to semiarid regions, the variance of the yearly long-term time series of (ii) and (iii) increase as local dryness decreases (not shown).

For the 12 subcatchments of the Tarim River basin, regions with ancient versus present towns are compared (see Table 1 and Fig. 7). Only the subcatchments Taklamakan (left), Qiemo, Kerriya, and Kongqi indicate significant abrupt changes in the time series of net radiation and excess water. The years with abrupt change or the tipping point are displayed and highlighted for the subcatchments. From the net radiation time series, the year 1957 for Taklamakan (left) and the year 1931 for Qiemo reveal abrupt changes, and for the excess water time series abrupt changes occur in the year 1925 for Kerriya. There is more than one abrupt changepoint in the confidence interval range for Kongqi. The first one appears in 1909, then several changepoints occur from the 1960s to 1970s (1961, 1964, 1966, 1971; see Fig. 7). The detected abrupt changes in annual excess water series coincide with the satellite-images-based prediction and may be one of the reasons why the lake is called a “wandering lake” (Hedin and Lyon 1940; Xia et al. 2007). For example, it was generally accepted that the lake was dry in 1972 based on Landsat Multispectral Scanner System (MSS) images. While the earliest aerial photographs (taken in 1958) showed that there was only a small area of water and that most of the lake was dry, and CORONA satellite images showed that the lake was dry in 1961 (Dong et al. 2012).

Streamflow and discharge into the closed basin of lake Lop Nur has been directly supplied by the Kongqi River, so excess water decreases of the Kongqi subcatchment before 1970s may lead to its final desiccation. Although the excess water of the Kongqi subcatchment increases after 1970s, the final desiccation is unstoppable. Besides the drier pattern (1941–60 versus 1961–80) shown in Fig. 5c, anthropogenic water withdrawal for irrigation farming in the middle reaches of rivers likely caused water shortage downstream and eventually the widespread deterioration of desert oases as the Aral Sea disaster (Mischke et al. 2017). In addition, the detected abrupt changes are in agreement with the conclusion that the closed basin of lake Lop Nur eventually desiccated until the 1970s (Hao et al. 2008; Hong et al. 2003; Hörner 1932; Qin et al. 2012).

4. Conclusions

The ecohydrological attribution model, first proposed by Tomer and Schilling (2009), is extended by including the ecohydrological state variables, their changes, and their resistance and resilience, which are important and suitable indices for sustainable management of water resources. By quantifying trajectories in a surface climate state space spanned by (U, W) coordinates, the ecohydrological conceptual model attributes the causes of change to 1) climate impact (in terms of precipitation and net radiation) as external forcing and 2) internal processes (induced by anthropogenic activities) that modify the partitioning of the related surface fluxes. However, the water and the heat storage deficits in the ecohydrological conceptual model are neglected so that the water demand and supply limits require steady-state conditions. The problem with the steady-state assumption is the leakage for how the large-scale evolutionary changes over time and whether and where do tipping points do occur during the evolutionary changes.

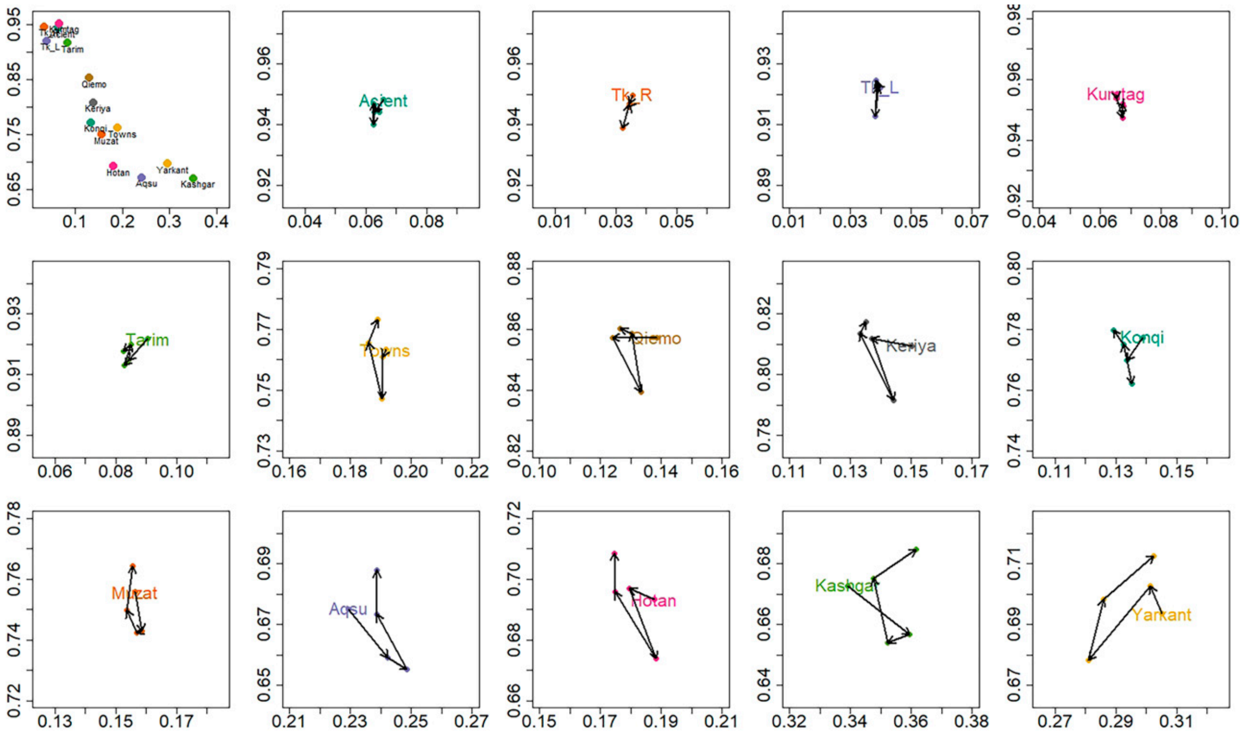

FIG. 6. Trajectories (U, W) changes are shown for the 12 subcatchments, regions with ancient relics vs present towns, with subsequent 20-yr time intervals starting from 1901 to 1920.

Changes in climate conditions and anthropogenic activities contribute to significant alterations in the ecohydrological patterns, causing dwindling in lake areas, degradation in water ecosystems and loss/fragmentation of natural habitats, particularly in arid regions (Xue et al. 2017). Lop Nur has long been considered a place of mystery. Its mystical qualities reached a peak in the 1980s, when satellite images revealed the depression's helical salt crust structure, a structure like a human ear. The helical salt crust structures appear to have formed as the lake shrank, but how and when they formed is unclear. Present predictions based on satellite images show clues about the time of the helical salt crust structures' appearance or the final desiccation without explaining how. Thereby assessing responses of hydrological systems to climate change and human activities and associating this assessment with three temporal scales helps improving our understanding of the shrinkage of Lop Nur and its final desiccation in the twentieth century.

Instead of establishing the statistical relationship between streamflow and climatic factors, and considering the ecohydrologic framework used here assumes that the storage change is negligible in the long term (decades scale or beyond) but not in the short term (e.g., annual scale), a comprehensive ecohydrological approach is designed 1) to detect hydroclimatic and ecohydrological resistance/resilience conditions on century scale, 2) to explore contributions of external/climate impact

TABLE 1. Statistics from Mann–Kendall test: p values less than 0.01 are in bold.

p value	Ancient	Taklamakan_R	Taklamakan_L	Kumtag	Tarim	towns	Qiemo	Keriya	Konqi	Muzat	Aqsu	Hotan	Kashgar	Yarkant
dW	0.702	0.683	0.718	0.741	0.942	0.808	0.910	0.406	0.963	0.955	0.901	0.570	0.832	0.967
dU	0.679	0.951	0.714	0.635	0.984	0.768	0.996	0.595	1.000	0.768	0.627	0.580	0.580	0.938
C	0.687	0.930	0.706	0.638	0.938	0.661	0.938	0.556	0.885	0.761	0.721	0.542	0.749	0.788
A	0.836	0.768	0.635	0.824	0.905	0.591	0.776	0.283	0.897	0.881	0.893	0.563	0.828	0.631
Ro	0.586	0.683	0.872	0.308	0.303	0.058	0.783	0.047	0.051	0.167	0.501	0.267	0.514	0.167
N	0.105	0.030	**0.006**	0.118	0.289	0.406	**0.001**	0.014	0.498	0.511	0.415	0.254	0.448	0.632
H	0.241	0.307	0.101	0.891	0.508	0.135	0.227	0.089	0.273	0.249	0.208	0.262	0.167	0.143
E	0.284	0.149	0.603	0.066	0.848	0.354	0.575	0.807	0.760	0.267	0.046	0.787	0.356	0.386
P	0.558	0.306	0.661	0.203	0.929	0.362	0.842	0.457	0.531	0.403	0.199	0.531	0.676	0.744
U	0.315	0.157	0.710	0.052	0.842	0.318	1.000	0.589	0.501	0.298	0.068	0.511	0.146	0.206
W	0.400	0.733	0.460	0.639	0.045	0.158	0.348	**0.004**	**0.002**	0.197	0.643	0.073	0.838	0.351

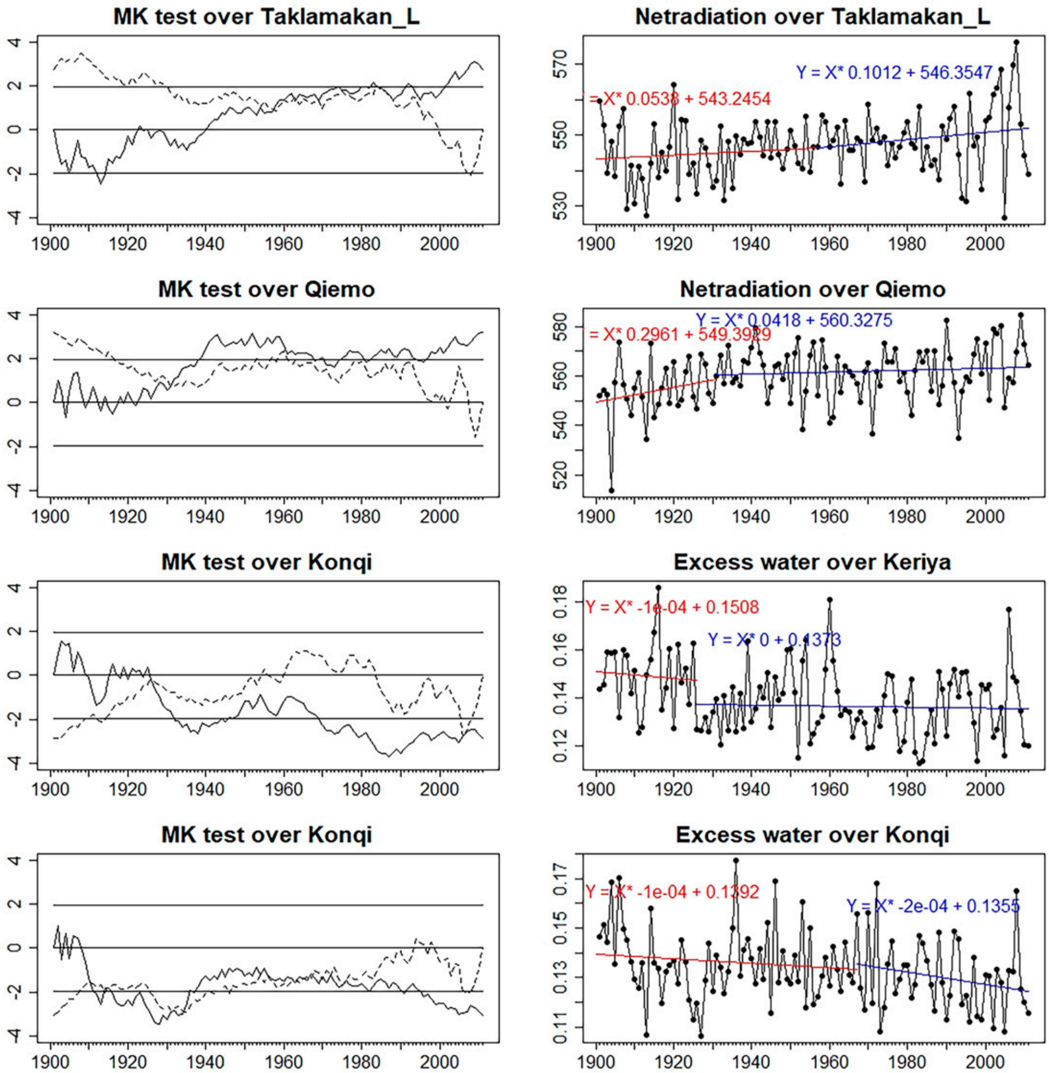

FIG. 7. Subcatchments of Taklamakan (left), Qiemo, Kerriya, and Kongqi indicate significant abrupt changes in the time series of net radiation and excess water.

or internal/anthropogenic activities on decadal scale, and 3) to identify tipping points in the yearly evolutionary processes. The following results are noted:

(i) The ancient towns and human settlements are located in arid regions, which have been abandoned for centuries, while the present towns are situated in regions with a natural hydraulic linkage with the mainstream of the Tarim River governed by semiarid conditions with dryness ratio around 2–3.

(ii) The arid regions with dryness ratios exceeding 3 (Taklamakan, Kumtag, Tarim, and ancient relics/towns, for example) show less sensitivity associated with low variabilities of excess water W and energy U and high resilience. That is, the desert is unlikely to be affected and will more likely stay in the same condition in the future.

(iii) Compared with the arid regions, the semiarid regions show relatively higher variabilities and lower possibility to which a catchment can return to normal after perturbations. That is, the semiarid regions are more sensitive and likely to be affected if drier scenarios occur in the future.

(iv) The attribution from two subsequent quasi-steady states provides a quantification of attribution to external or internal causes. Evidence points to the year 1960; before that, the Tarim River basin was getting wetter and then kept drying (see Fig. 5). Combined with the increase of the anthropogenic activities (Fig. 5d, 1961–80 versus 1981–2000), the results coincide with the conclusion that the closed-basin lake Lop Nur eventually desiccated until the 1970s (Hao et al. 2008; Hong et al. 2003; Hörner 1932; Qin et al. 2012) and is staying in this state.

(v) Streamflow and discharge into the closed basin of lake Lop Nur have been directly supplied by the Kongqi River, where the excess water time series indicates significant abrupt changes in the 1960s. Although the excess water time series has increased during in the post impacted period after decreasing in the preimpacted period, the final desiccation has been unstoppable, which is also in agreement with the recorded eventually desiccated lake Lop Nur in the 1970s (Hao et al. 2008; Hong et al. 2003; Hörner 1932; Qin et al. 2012).

In general, climate variables, flux ratios, and the external and internal influences in time and space are selected to explain the desiccation of Lop Nur. However, regional climate variations at various temporal and spatial scales are modulated by the variabilities of major climate modes, for example, El Niño–Southern Oscillation, North Atlantic Oscillation, and Atlantic multidecadal oscillation (Arpe et al. 2000; Zhang et al. 2017a,b). In a subsequent article we will comment on the anthropogenic modulation of catchments in the area around Lop Nor through specific land use changes as well as climate modes that could likely be responsible for some of the mentioned tipping points discovered here.

Acknowledgments. Support by the National Key Research and Development Project of China (Grant 2020YFC1521901 and 2020YFC1521904 in 2020YFC1521900), and by the Max Planck Fellow Group (DC, KF) is acknowledged.

Data availability statement. The subcatchments' boundary information as referred by Xu (2019) are downloadable from https://data.tpdc.ac.cn/zh-hans/. The ERA-20cm data are downloadable from https://apps.ecmwf.int/datasets/data/era20cm-edmo/levtype=sfc/.

REFERENCES

Arora, V. K., 2002: The use of the aridity index to assess climate change effect on annual runoff. *J. Hydrol.*, **265**, 164–177, https://doi.org/10.1016/S0022-1694(02)00101-4.

Arpe, K., L. Bengtsson, G. Golitsyn, I. Mokhov, V. Semenov, and P. Sporyshev, 2000: Connection between Caspian Sea level variability and ENSO. *Geophys. Res. Lett.*, **27**, 2693–2696, https://doi.org/10.1029/1999GL002374.

Boussetta, S., G. Balsamo, A. Beljaars, T. Kral, and L. Jarlan, 2013: Impact of a satellite-derived leaf area index monthly climatology in a global numerical weather prediction model. *Int. J. Remote Sens.*, **34**, 3520–3542, https://doi.org/10.1080/01431161.2012.716543.

Brutsaert, W., and M. Parlange, 1998: Hydrologic cycle explains the evaporation paradox. *Nature*, **396**, 30, https://doi.org/10.1038/23845.

Budyko, M., 1974: *Climate and Life.* Academic Press, 508 pp.

Cai, D., K. Fraedrich, F. Sielmann, L. Zhang, X. Zhu, S. Guo, and Y. Guan, 2015: Vegetation dynamics on the Tibetan Plateau (1982 to 2006): An attribution by eco-hydrological diagnostics. *J. Climate*, **28**, 4576–4584, https://doi.org/10.1175/JCLI-D-14-00692.1.

——, ——, ——, Y. Guan, and S. Guo, 2016: Land-cover characterization and aridity changes of South America (1982–2006): An attribution by ecohydrological diagnostics. *J. Climate*, **29**, 8175–8189, https://doi.org/10.1175/JCLI-D-16-0024.1.

Carey, S. K., and Coauthors, 2010: Inter-comparison of hydro-climatic regimes across northern catchments: Synchronicity, resistance and resilience. *Hydrol. Processes*, **24**, 3591–3602, https://doi.org/10.1002/hyp.7880.

Changchun, X., C. Yaning, L. Weihong, C. Yapeng, and G. Hongtao, 2008: Potential impact of climate change on snow cover area in the Tarim River basin. *Environ. Geol.*, **53**, 1465–1474, https://doi.org/10.1007/s00254-007-0755-1.

Chen, X., N. Alimohammadi, and D. Wang, 2013: Modeling interannual variability of seasonal evaporation and storage change based on the extended Budyko framework. *Water Resour. Res.*, **49**, 6067–6078, https://doi.org/10.1002/wrcr.20493.

Chen, Y., W. Li, C. Xu, and X. Hao, 2007: Effects of climate change on water resources in Tarim River Basin, northwest China. *J. Environ. Sci.*, **19**, 488–493, https://doi.org/10.1016/S1001-0742(07)60082-5.

Chen, Z., Y. Chen, W. Li, and Y. Chen, 2011: Changes of runoff consumption and its human influence intensity in the mainstream of Tarim River. *Acta Geogr. Sin.*, **66**, 89–98, https://doi.org/10.11821/xb201101009.

Creed, I. F., and Coauthors, 2014: Changing forest water yields in response to climate warming: Results from long-term experimental watershed sites across North America. *Global Change Biol.*, **20**, 3191–3208, https://doi.org/10.1111/gcb.12615.

Dong, Z., P. Lv, G. Qian, X. Xia, Y. Zhao, and G. Mu, 2012: Research progress in China's Lop Nur. *Earth-Sci. Rev.*, **111**, 142–153, https://doi.org/10.1016/j.earscirev.2011.11.003.

Esquivel-Hernández, G., R. Sánchez Murillo, C. Birkel, S. P. Good, and J. Boll, 2017: Hydroclimatic and ecohydrological resistance/resilience conditions across tropical biomes of Costa Rica. *Ecohydrology*, **10**, e1860, https://doi.org/10.1002/eco.1860.

Fraedrich, K., 2010: A parsimonious stochastic water reservoir: Schreiber's 1904 equation. *J. Hydrometeor.*, **11**, 575–578, https://doi.org/10.1175/2009JHM1179.1.

Greve, P., L. Gudmundsson, B. Orlowsky, and S. I. Seneviratne, 2016: A two-parameter Budyko function to represent conditions under which evapotranspiration exceeds precipitation. *Hydrol. Earth Syst. Sci.*, **20**, 2195–2205, https://doi.org/10.5194/hess-20-2195-2016.

Hao, X., Y. Chen, C. Xu, and W. Li, 2008: Impacts of climate change and human activities on the surface runoff in the Tarim River Basin over the last fifty years. *Water Resour. Manage.*, **22**, 1159–1171, https://doi.org/10.1007/s11269-007-9218-4.

Hedin, S. A., 1925: *My Life as an Explorer.* Garden City Publishing Company, 544 pp.

——, and F. H. Lyon, 1940: *The Wandering Lake.* E.P. Dutton, 291 pp.

Hersbach, H., C. Peubey, A. Simmons, P. Berrisford, P. Poli, and D. Dee, 2015: ERA-20CM: A twentieth-century atmospheric model ensemble. *Quart. J. Roy. Meteor. Soc.*, **141**, 2350–2375, https://doi.org/10.1002/qj.2528.

Hong, Z., W. Jian-Wei, Z. Qiu-Hong, and Y. Yun-Jiang, 2003: A preliminary study of oasis evolution in the Tarim Basin, Xinjiang, China. *J. Arid Environ.*, **55**, 545–553, https://doi.org/10.1016/S0140-1963(02)00283-5.

Hörner, N. G., 1932: Lop-Nor: Topographical and geological summary. *Geogr. Ann.*, **14**, 297–321, https://doi.org/10.2307/519598.

Leiwen, J., T. Yufen, Z. Zhijie, L. Tianhong, and L. Jianhua, 2005: Water resources, land exploration and population dynamics in arid areas-the case of the Tarim River basin in Xinjiang of China. *Popul. Environ.*, **26**, 471–503, https://doi.org/10.1007/s11111-005-0008-8.

Libiseller, C., and A. Grimvall, 2002: Performance of partial Mann–Kendall tests for trend detection in the presence of covariates. *Environmetrics*, **13**, 71–84, https://doi.org/10.1002/env.507.

Mann, H. B., 1945: Nonparametric tests against trend. *Econometrica*, **13**, 245–259, https://doi.org/10.2307/1907187.

Mischke, S., C. Liu, J. Zhang, C. Zhang, H. Zhang, P. Jiao, and B. Plessen, 2017: The world's earliest Aral-Sea type disaster: The decline of the Loulan Kingdom in the Tarim Basin. *Sci. Rep.*, **7**, 43102, https://doi.org/10.1038/srep43102.

——, ——, and ——, 2020: Lop Nur in NW China: Its natural state, and a long history of human impact. *Large Asian Lakes in a Changing World*, Springer, 207–234.

Orlowsky, B., and S. I. Seneviratne, 2013: Elusive drought: Uncertainty in observed trends and short- and long-term CMIP5 projections. *Hydrol. Earth Syst. Sci.*, **17**, 1765–1781, https://doi.org/10.5194/hess-17-1765-2013.

Potter, N., and L. Zhang, 2007: Water balance variability at the interstorm timescale. *Water Resour. Res.*, **43**, W05405, https://doi.org/10.1029/2006WR005276.

Qin, X., and Coauthors, 2012: New evidence of agricultural activity and environmental change associated with the ancient Loulan kingdom, China, around 1500 years ago. *Holocene*, **22**, 53–61, https://doi.org/10.1177/0959683611405234.

Renner, M., R. Seppelt, and C. Bernhofer, 2012: Evaluation of water-energy balance frameworks to predict the sensitivity of streamflow to climate change. *Hydrol. Earth Syst. Sci.*, **16**, 1419–1433, https://doi.org/10.5194/hess-16-1419-2012.

Roderick, M. L., and G. D. Farquhar, 2011: A simple framework for relating variations in runoff to variations in climatic conditions and catchment properties. *Water Resour. Res.*, **47**, W00G07, https://doi.org/10.1029/2010WR009826.

Szilagyi, J., 2007: On the inherent asymmetric nature of the complementary relationship of evaporation. *Geophys. Res. Lett.*, **34**, L02405, https://doi.org/10.1029/2006GL028708.

Tomer, M. D., and K. E. Schilling, 2009: A simple approach to distinguish land-use and climate-change effects on watershed hydrology. *J. Hydrol.*, **376**, 24–33, https://doi.org/10.1016/j.jhydrol.2009.07.029.

Wang, D., and M. Hejazi, 2011: Quantifying the relative contribution of the climate and direct human impacts on mean annual streamflow in the contiguous United States. *Water Resour. Res.*, **47**, 10283, https://doi.org/10.1029/2010WR010283.

——, and N. Alimohammadi, 2012: Responses of annual runoff, evaporation, and storage change to climate variability at the watershed scale. *Water Resour. Res.*, **48**, W05546, https://doi.org/10.1029/2011WR011444.

Wang, G., 2005: Agricultural drought in a future climate: Results from 15 global climate models participating in the IPCC 4th assessment. *Climate Dyn.*, **25**, 739–753, https://doi.org/10.1007/s00382-005-0057-9.

Xia, X., F. Wang, and Y. Zhao, 2007: *China Lop Nur.* Science Press, 482 pp.

Xu, C., Y. Chen, Y. Chen, R. Zhao, and H. Ding, 2013: Responses of surface runoff to climate change and human activities in the arid region of Central Asia: A case study in the Tarim River Basin, China. *Environ. Manage.*, **51**, 926–938, https://doi.org/10.1007/s00267-013-0018-8.

Xu, M., 2019: The Tarim River Basin boundary (2019). National Tibetan Plateau Data Center, https://data.tpdc.ac.cn/en/data/d5acb79d-8ffe-494e-8081-79938d2cb1fe/.

Xu, Z., Z. Liu, G. Fu, and Y. Chen, 2010: Trends of major hydroclimatic variables in the Tarim River basin during the past 50 years. *J. Arid Environ.*, **74**, 256–267, https://doi.org/10.1016/j.jaridenv.2009.08.014.

Xue, L., F. Yang, C. Yang, X. Chen, L. Zhang, Y. Chi, and G. Yang, 2017: Identification of potential impacts of climate change and anthropogenic activities on streamflow alterations in the Tarim River Basin, China. *Sci. Rep.*, **7**, 8254, https://doi.org/10.1038/s41598-017-09215-z.

Yang, X., and X. Lu, 2014: Drastic change in China's lakes and reservoirs over the past decades. *Sci. Rep.*, **4**, 6041, https://doi.org/10.1038/srep06041.

——, Z. Liu, F. Zhang, P. White, and X. Wang, 2006: Hydrological changes and land degradation in the southern and eastern Tarim Basin, Xinjiang, China. *Land Degrad. Dev.*, **17**, 381–392, https://doi.org/10.1002/ldr.744.

Ye, M., H. Xu, and Y. Song, 2006: The utilization of water resources and its variation tendency in Tarim River Basin. *Chin. Sci. Bull.*, **51**, 16–24, https://doi.org/10.1007/s11434-006-8203-2.

Zhang, F., Y. Lei, Q.-R. Yu, K. Fraedrich, and H. Iwabuchi, 2017a: Causality of the drought in the southwestern United States based on observations. *J. Climate*, **30**, 4891–4896, https://doi.org/10.1175/JCLI-D-16-0601.1.

——, P. Yang, K. Fraedrich, X. Zhou, G. Wang, and J. Li, 2017b: Reconstruction of driving forces from nonstationary time series including stationary regions and application to climate change. *Physica A*, **473**, 337–343, https://doi.org/10.1016/j.physa.2016.12.088.

Zhang, J., W. GuiHua, W. QiMeng, and L. XiaoYan, 2010: Restoring environmental flows and improving riparian ecosystem of Tarim River. *J. Arid Land*, **2**, 43–50.

Zhang, L., N. Potter, K. Hickel, Y. Zhang, and Q. Shao, 2008: Water balance modeling over variable time scales based on the Budyko framework–Model development and testing. *J. Hydrol.*, **360**, 117–131, https://doi.org/10.1016/j.jhydrol.2008.07.021.